

**RESEARCH ARTICLE**

# Optimal Operation of a Grid-Connected Battery Energy Storage System Over its Lifetime<sup>†</sup>

Ioannis Kordonis\*<sup>1</sup> | Alexandros C. Charalampidis<sup>1,2</sup> | Pierre Haessig<sup>1</sup>

<sup>1</sup> IETR (Institut d'Électronique et de Télécommunications de Rennes) – CentraleSupélec, Avenue de la Boulaie, 35576 Cesson-Sévigné, France

<sup>2</sup> Department of Electrical Engineering and Computer Science, Control Systems Group, Technische Universität Berlin, Einsteinufer 17, Berlin D-10587, Germany

**Correspondence**

\* Email: jkordonis1920@yahoo.com

**Summary**

This paper deals with the optimal control of grid-connected Battery Energy Storage Systems (BESSs) operating for energy arbitrage. An important issue is that BESSs degrade over time, according to their use, and thus they are usable only for a limited number of cycles. Therefore, the time horizon of the optimization depends on the actual operation of the BESS. We focus on Li-ion batteries and use an empirical model to describe battery degradation. The BESS model includes an equivalent circuit for the battery and a simplified model for the power converter. For the price, we use a linear stochastic model, including the effect of the time-of-the-day. The problem of maximizing the revenues obtained over the BESS lifetime is formulated as a stochastic optimal control problem with a long, operation-dependent time horizon. First, we divide this problem into a finite set of sub-problems, such that for each one of them, the State of Health (SoH) of the battery is approximately constant. Next, we reformulate approximately every sub-problem into the minimization of the ratio of two long-time average-cost criteria and use a value-iteration-type algorithm to derive the optimal policy. Finally, we present some numerical results. It turns out that the optimal policy is more aggressive for a more aged battery. We also investigate the effects of the energy loss parameters, degradation parameters, and price on the optimal policy.

**KEYWORDS:**

Battery Energy Storage Systems (BESSs), Battery degradation, Stochastic optimal control, Ratio cost problems, Dynamic Programming

## 1 | INTRODUCTION

Battery Energy Storage Systems (BESSs) gain ground in the power system, as means to mitigate the uncertainties caused by the increased penetration of renewable sources. BESS could have various roles in the power grid, including load shifting, energy arbitrage (buy energy when the price is low and sell it back when the price is high), frequency regulation, and improving power quality in microgrids. Among the various battery technologies, Li-ion batteries are becoming increasingly competitive for static

<sup>†</sup>This work has been supported by the Regional Council of Brittany (SAD 2016 - REINMASE, 9693) and People Programme (Marie Curie Actions) of the European Union's Seventh Framework Programme (FP7/2007-2013) under REA grant agreement n. PCOFUND-GA-2013-609102, through the PRESTIGE programme coordinated by Campus France. The work of A. C. Charalampidis has been also supported by the European Union's Horizon 2020 research and innovation programme under the Marie Skłodowska-Curie grant agreement No 705982.

Authors' emails: I. Kordonis jkordonis1920@yahoo.com, A.C. Charalampidis: alexandros.charalampidis@centralesupelec.fr, P. Haessig: pierre.haessig@centralesupelec.fr.

solutions. Despite the sharp decline in battery prices during recent years<sup>1,2</sup>, investment costs remain still high. Furthermore, batteries degrade (age) over time, according to their use, and degradation eventually leads to the end of their useful life (EoL). Thus, it is important to optimize the operation of BESSs over their lifetime, which is, however, operation-dependent.

Battery degradation is a complex nonlinear phenomenon caused by irreversible chemical and mechanical variations of the battery materials. In the current work, we focus on Li-ion batteries. For a review of the degradation mechanisms of Li-ion batteries, see Vetter et al. (2005)<sup>3</sup>. There are two kinds of models for battery aging: empirical and physics-based models. Physics-based models<sup>4,5,6</sup> are able to make the most accurate predictions but involve coupled PDEs. Thus, it is difficult to use them to optimize battery operation. Most of the papers studying the optimal operation of BESSs use simple empirical models. In this article, we use a detailed empirical model<sup>7</sup>, capturing many aspects of battery degradation. An alternative model can be found in Suri et al. (2016)<sup>8</sup>.

Usually, battery degradation is included in the optimization of BESS operation using a simplifying assumption. Several articles<sup>9,10,11,12,13,14</sup> assume that there is a certain cost for the use of the battery, proportional to the initial investment cost. Another approach is to put certain constraints on battery usage<sup>15,16,17</sup>. Other authors use separation of time scales ideas<sup>18,19,20</sup>. However, most of the approaches do not consider the impact of BESS usage on the time horizon of the problem. Notable exceptions are the works of Tan et al.<sup>21,22</sup>, where the problem is formulated as a Stochastic Shortest Path (SSP) problem. In order to do so, however, the state space should be extended to include the total degradation up to the current time step. This extension leads to huge state space cardinalities and makes the analysis and optimization of detailed models computationally challenging.

In this paper, we optimize the long-term profits of a BESS, operating for energy arbitrage. We build on our previous work<sup>23</sup>, which considered an ampere-hour counting (empirical) model for battery degradation and a simplified electrical model for the battery. In that paper, we reformulated a problem with a long, operation-dependent time horizon into the problem of minimizing the ratio of two long-time average-cost criteria. In this article, we use more accurate (nonlinear and non-convex) electrical and battery degradation models. For these models, the method developed in our previous work<sup>23</sup> is not directly applicable. The problem is that the degradation rate depends on the battery's State of Health (SoH). To overcome this difficulty, we divide the SoH state into small parts and apply the methods developed in that paper into each of these intervals.

This reformulation leads to Bellman-type equations for each subdivision of the SoH. To solve these equations, we develop a value-iteration-type algorithm for ratio objective problems with a periodic Markov chain. Numerical results indicate that, as the BESS becomes older, the optimal policy becomes more aggressive. We then analyze the effects of the price dynamics, the electrical and the aging parameters on the optimal control law.

In summary, the contribution of this work is fourfold:

- (a) We develop a detailed (nonlinear non-convex) model to describe the optimal operation of a BESS over its lifetime.
- (b) We reformulate this problem in terms of a set of ratio cost problems that are much easier to solve.
- (c) We propose an efficient value-iteration-type algorithm to solve these problems.
- (d) We provide some numerical results for the BESS optimal control problem and investigate the effect of the different parameters on the optimal control law.

The rest of this paper is organized as follows. In Section 2, we describe an electrical model for the BESS and a model for battery degradation. Furthermore, a stochastic model of the price dynamics is presented. Section 3 presents a stochastic optimal control problem formulation, describing the revenue maximization of a BESS operating for energy arbitrage. Section 4 reformulates the original problem into a set of ratio-cost problems and describes an algorithm for solving them. Section 5 presents the numerical results, and in Section 6, we review the basic contributions of the current work.

## 2 | MATHEMATICAL MODEL

### 2.1 | Electrical Model

This section describes a model of a grid-connected BESS (Figure 1). The battery pack is connected to the grid through a bidirectional inverter. To model the battery pack, we use the Equivalent Circuit Model (ECM) of Figure 2 (see e.g. Plett (2015)<sup>24</sup>), which consists of an ideal voltage source, a nonlinear hysteresis element and a resistor  $R$ .

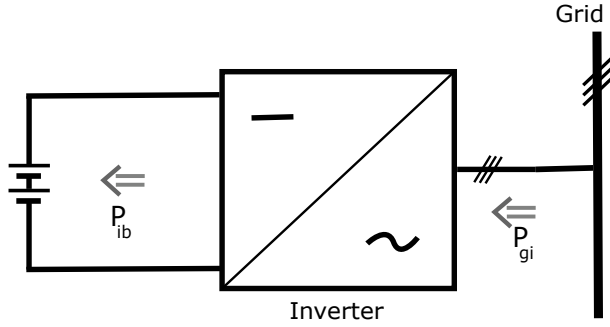


**FIGURE 1** A schematic representation of the BESS. The battery pack is connected to the grid through a bidirectional DC-AC power converter.

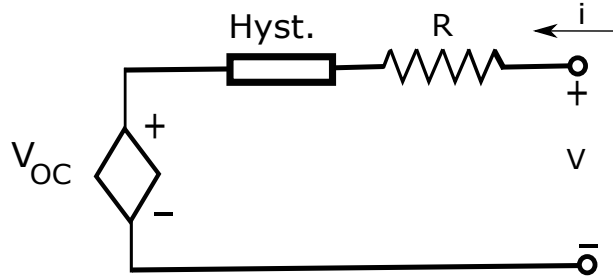


**FIGURE 2** Equivalent circuit model. It consists of an ideal voltage source a hysteresis element and a resistor.

The voltage  $V$  at the terminals of the battery pack is given by:

$$V = V_{OC} + Ri + \text{sgn}(i)V_h,$$

where  $V_{OC}$  is the open circuit voltage,  $V_h$  is the hysteresis voltage,  $i$  is the current from the inverter to the battery pack, and  $\text{sgn}(i)$  is given by:

$$\text{sgn}(i) = \begin{cases} 1 & \text{if } i > 0 \\ 0 & \text{if } i = 0 \\ -1 & \text{if } i < 0 \end{cases}.$$

Let us note that the value of the open circuit voltage  $V_{OC}$  may depend on the State of Charge.

The State of Charge  $\text{SoC} \in [0, 1]$ , of the battery evolves according to:

$$\frac{d}{dt} \text{SoC} = \frac{1}{C} i, \quad (1)$$

where  $C$  is the capacity of the battery.

The power  $P_{ib}$ , flowing from the inverter to the battery, is given by:

$$P_{ib} = Vi = V_{OC}i + Ri^2 + |i|V_h.$$

The power losses of the inverter can be expressed as a function of  $P_{ib}$  as  $P_{\text{InvLoss}}(P_{ib})$ . Thus the power flowing from the grid to the BESS is given by:

$$P_{gi} = f_{P_{gi}}(i) = P_{ib} + P_{\text{InvLoss}}(P_{ib}). \quad (2)$$

*Remark 1.* More detailed models for the battery or the power converter could be used. For example, the ECM could contain an RC element (modeling diffusion voltage). We chose the presented models for the battery and the converter because they provide a reasonable approximation of the energy conversion. Let us note that most of the literature presents more simplified models.

## 2.2 | Battery Degradation Model

Batteries degrade over time due to several different mechanisms. Some of them are related to cycling (cycling aging) and others to time pass (calendar aging)<sup>25</sup>. There is a variety of battery degradation models in the literature. Furthermore, degradation depends on the particular battery chemistry<sup>26</sup>. The methods presented in this paper are applicable to any macroscopic model which depends on the battery current, voltage and SoC. In this section, we describe a simplified version of the battery aging model presented in Petit et al. (2016)<sup>7</sup>, which is an rather detailed empirical model, capturing many aspects of battery degradation.

The degradation  $Q$  of the battery is expressed in terms of the capacity loss as:

$$Q(t) = \frac{C(0) - C(t)}{C(0)},$$

where  $C(t)$  is the capacity of the battery at time  $t$ . The degradation  $Q$  evolves over time according to the differential equation:

$$\dot{Q} = f^{\text{cal}}(Q, \text{SoC}) + f^{\text{cyc}}(Q, I) \quad (3)$$

and where  $I$  is the C-rate i.e.,  $I = i/C$  and  $f^{\text{cal}}(Q, \text{SoC})$  and  $f^{\text{cyc}}(Q, I)$  are given by:

$$f^{\text{cal}}(Q, \text{SoC}) = (c_1 + c_2 \text{SoC})Q^{-c_3}, \quad (4)$$

$$f^{\text{cyc}}(Q, I) = |I|c_4 Q^{-c_5} e^{c_6 |I|}, \quad (5)$$

for appropriate positive constants  $c_1, \dots, c_6$ .

This model captures the following characteristics of battery aging:

- (i) Batteries degrade faster in the initial period of their life.
- (ii) Aging depends both on the time pass and the battery use.
- (iii) The use of large currents makes the batteries degrade faster.
- (iv) Storing batteries with high SoC accelerates aging.

The EoL of the battery is described by a maximum degradation  $Q_M$ . A reasonable value for  $Q_M$  could be 0.2 or 0.3<sup>25</sup>.

*Remark 2.* An interesting extension would be to include battery temperature, using a thermal model, or consider the increase in the internal resistance.

## 2.3 | Model Discretization

The BESS participates in an energy market, which operates in discrete time intervals  $\Delta t$  (e.g. 1 hour or 15 minutes). We thus discretize the model, and assume that the power from or to the BESS is constant during each interval  $\Delta t$ . The discrete time version of (1) is given by:

$$\text{SoC}_{k+1} = \text{SoC}_k + u_k, \quad (6)$$

where the control variable  $u_k$  is given by  $u_k = \frac{i\Delta t}{C_k}$ . For the control action  $u_k$  there is a constraint:

$$u_k \in [-u_M, u_M] \cap [-\text{SoC}_k, 1 - \text{SoC}_k] \quad (7)$$

representing that there is a maximum and minimum charging rate and that the SoC cannot drop below 0 or rise above 1.

Battery aging is a much slower phenomenon compared to charging/discharging. Thus, we can discretize the degradation dynamics with a very small error as:

$$\begin{aligned} Q_{k+1} &= Q_k + \Delta t (f^{\text{cal}}(Q_k, \text{SoC}_k) + f^{\text{cyc}}(Q_k, u_k/\Delta t)) \\ &= Q_k + g_2(Q_k, \text{SoC}_k, u_k), \end{aligned} \quad (8)$$

where we used that  $I = u_k/\Delta t$ . The function  $g_2(Q_k, \text{SoC}_k, u_k)$  expresses the degradation rate of the BESS and it is computed using (4), (5).

## 2.4 | Energy Arbitrage and Price Model

The revenue of the BESS depends on the energy price. We assume that the effects of the BESS in the power grid are small and thus we treat the price as an external signal. Since future prices are uncertain, the price will be modeled as a random process.

Denoting by  $p_k$  the price during time interval  $k$ , the cost for the energy exchange during that interval is:

$$g_1(Q_k, p_k, u_k) = p_k f_{P_{\text{gi}}}(C_k u_k / \Delta t) \Delta t, \quad (9)$$

where  $f_{P_{\text{gi}}}$  is the power flowing from the grid to the BESS given in (2).

We assume that the price  $p_k$  depends on the time-of-the-day  $t_k$  as follows:

$$p_k = \bar{p}(t_k) + \tilde{p}_k, \quad (10)$$

where  $\bar{p}(t_k)$  is the mean price at time  $t_k$ , and  $\tilde{p}_k$  is the detrended (deseasonalized) price. We model the evolution of the deseasonalized price  $\tilde{p}_k$  as a first order time invariant linear dynamics with a random disturbance  $w_k$ :

$$\tilde{p}_{k+1} = \alpha \tilde{p}_k + w_k, \quad (11)$$

where  $0 < \alpha < 1$ .

The time-of-the-day evolves according to:

$$t_{k+1} = (t_k + \Delta t) (\text{mod } 24h). \quad (12)$$

## 3 | PROBLEM FORMULATION

In this section, we first discretize the state space of the model and introduce some notation necessary for the rest of the paper. Then, we formulate a stochastic optimal control problem describing the maximization of the revenue obtained over the BESS lifetime.

### 3.1 | State Space Discretization

The state space consists of the fast varying state variables  $\text{SoC}_k, \tilde{p}_k, t_k$  and the slowly varying degradation variable  $Q_k$ . We now discretize the fast varying variables of the state space. We denote by  $x^1, x^2, x^3$  and  $u$  the discrete values of the state variables  $\text{SoC}_k, \tilde{p}_k, t_k$  and the control input, taking values in  $X^1, X^2, X^3$ , and  $U$  respectively.

Denote the vector of fast varying state variables  $[x_k^1, x_k^2, x_k^3]$  by  $x_k$ . Denote also by  $X = X^1 \times X^2 \times X^3$  the state space of  $x$  and by  $F(x)$  the feasible subset of the discrete action space, i.e., the values of  $u$  satisfying (7). Assume that the time-of-the-day state space  $X_3$ , consists of  $v_3 + 1$  points, indexed as  $0, 1, \dots, v_3$  and that  $X$  consists of  $v$  points.

In compact form the dynamics is written as:

$$x_{k+1} = f(x_k, u_k, w_k). \quad (13)$$

It is convenient to use the controlled Markov chain notation  $P(x_{k+1} = j | x_k = i, u_k = u) = p_{ij}(u)$  to describe the stochastic dynamics (13).

### 3.2 | Optimal Control Problem

We then describe the optimal control problem as the minimization of the cumulative cost of the BESS over its lifetime (or equivalently as the maximization of the revenues over the lifetime). The lifetime is a random variable (stopping time) given by:

$$T = \min\{k : Q_k \geq Q_M\}. \quad (14)$$

Then the problem of optimal operation is given by:

$$\text{minimize } J_a = E \left[ \sum_{k=0}^T g_1(x_k, Q_k, u_k) \right], \quad (15)$$

where the minimization is considered on the set of memory-less feasible policies of the form  $u_k = \mu(x_k, Q_k)$ .

This is a Stochastic Shortest Path (SSP) problem<sup>27</sup>. Namely, it is a stochastic optimal control problem, for which we consider as absorbing states the tuples  $(x_k, Q_k)$  satisfying  $Q_k \geq Q_M$ . The time horizon  $T$  depends both on the control law and the realization of the random variables  $w_k$ .

There are some Dynamic Programming algorithms for this kind of problems in the literature. However, the inclusion of the degradation variable  $Q_k$  into the state space makes its cardinality very large, and thus the corresponding computations very demanding. In the following section, we present a reformulation of this problem which leads to more efficient computations.

## 4 | PROBLEM REFORMULATION AND SOLUTION ALGORITHM

In this section we present an approximate reformulation of the problem which leads to a set of optimization problems involving the ratio of two long-time average-cost problems. Then, we present a solution algorithm, for each of these problems, which takes into account the periodic structure of the model.

### 4.1 | Problem Reformulation

Problem (15) is not easy to solve, due to its long and operation-dependent time horizon. We then provide a series of approximate reformulations of (15), leading eventually to a set of ratio cost problems that are easier to solve. The first step is to divide the time horizon into a number of pieces according to the battery degradation state. Particularly, the cost function can be expressed as:

$$J_a = J_a^1 + \dots + J_a^N,$$

where:

$$J_a^n = E \left[ \sum_{k=T_{n-1}+1}^{T_n} g_1(x_k, Q_k, u_k) \right], \quad (16)$$

$T_0 = -1$  and  $T_n$  is a stopping time describing the first instant of time where  $Q_k \geq nQ_M/N$ . That is:

$$T_n = \min\{k : Q_k \geq nQ_M/N\}.$$

In other words, the time horizon is sliced in  $N$  pieces, according to the state of degradation  $Q$ . Note that the times of slicing  $T_n$  are not pre-specified and depend on the control law and the randomness realization.

We approximate the optimal control law for  $J_a$  with the control law which is optimal for each  $J_a^n$ .

*Remark 3.* The minimization of  $J_a^n$  in (16) ignores the effects that the final condition  $(x_{T_n}^1, x_{T_n}^2, Q_{T_n})$  has on  $J_a^{n+1}$ . Thus, the quality of this approximation depends on the degree of dependence of  $J_a^{n+1}$  on its initial conditions  $(x_{T_n+1}^1, x_{T_n+1}^2, Q_{T_n+1})$ . Since the time horizon of each of the problems  $J_a^1, \dots, J_a^N$  is long, we expect that the dependence on the initial conditions will be small.

Observe that the degradation dynamics is much slower than the everyday operation. If  $N$  is large enough, the value of  $Q_k$  is almost constant in each of the intervals  $[T_{n-1}, T_n]$ . We take this value to be  $\bar{Q}_n = (n - 1/2)Q_M/N$ . Thus, in the  $n$ -th interval the optimal control problem is approximately reformulated as:

$$\underset{u_k=\mu_k(x_k)}{\text{minimize}} \quad J_b^n = E \left[ \sum_{k=0}^{\bar{T}_n} g_1(x_k^2, \bar{Q}_n, u_k) \right]. \quad (17)$$

where  $\bar{T}_n = \min\{\tau : \sum_{k=0}^{\tau} g_2(x_k, u_k, \bar{Q}_n) \geq Q_M/N\}$ .

Note that in the optimal control problem (17), the state is  $(x_k^1, x_k^2, x_k^3) \in X$  and the degradation variable is not a part of the state.

*Remark 4.* There is a trade-off in the choice of  $N$ . We need  $N$  to be large enough so that  $Q_k$  does not vary much in each interval. On the other hand, the value of  $N$  should not be too high, for the problems  $J_a^1, \dots, J_a^N$  to have a long horizon (see Remark 3). Furthermore, a large value of  $N$  would result in a large number of computations. In the numerical examples, we will use  $N = 30$ .

We then provide the final approximate reformulation of our problem. The cost function  $J_b^n$  in (17) will be approximated by a ratio cost  $J_c^n$ , given by:

$$J_c^n = \frac{Q_M}{N} \frac{J_{c,\text{num}}^n}{J_{c,\text{den}}^n}, \quad (18)$$

where the cost functions in the numerator and the denominator are long-time average-cost criteria:

$$J_{c,\text{num}}^n = \lim_{T_d \rightarrow \infty} E \left[ \frac{1}{T_d} \sum_{k=0}^{T_d} g_1^n(x_k, u_k) \right], \quad (19)$$

$$J_{c,\text{den}}^n = \lim_{T_d \rightarrow \infty} E \left[ \frac{1}{T_d} \sum_{k=0}^{T_d} g_2^n(x_k, u_k) \right], \quad (20)$$

where  $g_1^n(x_k, u_k) = g_1(x_k, \bar{Q}_n, u_k)$ ,  $g_2^n(x_k, u_k) = g_2(\bar{Q}_n, x_k^1, u_k)$ ,  $g_2$  is given in (8), and  $T_d$  is deterministic. For a policy  $\mu$ , the value of  $J_{c,\text{num}}^n$  represents the cost rate (minus the revenue rate) and the value of  $J_{c,\text{den}}^n$  represents the degradation rate.

*Remark 5.* The intuition behind the last approximation is the following. The total cost  $J_b^n$  is approximated by the average cost per stage  $J_{c,\text{num}}^n$  times the number of states  $T_n$ . On the other hand, the number of stages is inversely proportional to the average degradation per stage  $J_{c,\text{den}}^n$ .

The following proposition shows that if a policy  $\mu$  minimizes (18), then it is also minimizing (17) approximately. It provides also a characterization of the optimal policy of (17), in terms of Bellman-type equations. This characterization will be used to derive a solution algorithm.

**Proposition 1** (Results from Koronis et al.<sup>23</sup>). It holds:

(a) Consider the optimal control problem:

$$\underset{u_k=\mu(x_k)}{\text{minimize}} J_c^n, \quad (21)$$

and denote by  $\mu^{\star,n}(\cdot)$  the optimal control law. Then, provided that the aging is slow, i.e., that the constants  $c_1$ ,  $c_2$ , and  $c_4$  are small enough, the policy  $\mu^{\star,n}(\cdot)$  is  $\varepsilon$ -optimal for (17).

(b) Assume that there exist constants  $\lambda_1^{\star,n}, \lambda_2^{\star,n}$ , vectors  $h_1^{\star,n}, h_2^{\star,n} \in \mathbb{R}^v$ , and a policy  $\mu^{\star,n}$  such that:

$$\lambda_1^{\star,n} + h_1^{\star,n}(i) = g_1^n(i, \mu^{\star,n}(i)) + \sum_{j=1}^v h_1^{\star,n}(j) p_{ij}(\mu^{\star,n}(i)) \quad (22)$$

$$\lambda_2^{\star,n} + h_2^{\star,n}(i) = g_2^n(i, \mu^{\star,n}(i)) + \sum_{j=1}^v h_2^{\star,n}(j) p_{ij}(\mu^{\star,n}(i)) \quad (23)$$

$$\mu^{\star,n}(i) = \underset{u \in F(i)}{\text{argmin}} \left[ \lambda_2^{\star,n} g_1^n(i, u) - \lambda_1^{\star,n} g_2^n(u) + \sum_{j=1}^v p_{ij}(u) (\lambda_2^{\star,n} h_1^{\star,n}(j) - \lambda_1^{\star,n} h_2^{\star,n}(j)) \right]. \quad (24)$$

for all  $i \in X$ . Then,  $\lambda^{\star,n} = \lambda_1^{\star,n}/\lambda_2^{\star,n}$  is the optimal value of (18) and the minimizer  $u = \mu^{\star,n}(i)$  of (24) is the optimal control law. Furthermore, the controller  $u = \mu^{\star,n}(i)$  is optimal for the long-time average-cost criterion:

$$\lim_{T_d \rightarrow \infty} \frac{1}{T_d} E \left[ \sum_{k=0}^{T_d} r^n(x_k, u_k) \right] \quad (25)$$

where  $r^n(x_k, u_k) = \lambda_2^{\star,n} g_1^n(i, u) - \lambda_1^{\star,n} g_2^n(u)$  and the value of this cost is 0.  $\square$

Equations (22) and (23) are the Bellman equations for the long-time average-cost criteria  $J_{c,\text{num}}^n$  and  $J_{c,\text{den}}^n$ , under the policy  $\mu^{\star,n}$ . Equation (24) represents that  $\mu^{\star,n}$  minimizes (25).

It turns out that problem (21) is easier to solve numerically. Having characterized the optimal solution for (21), in the following subsection we propose an efficient algorithm based on value iteration.

## 4.2 | Solution Algorithm

We then develop a value-iteration-type algorithm on each one of the problems in the form (21). This algorithm is a modification of the one presented in our previous work<sup>23</sup> using the fact that the controlled Markov chain (13) is periodic.

Let us partition the state space  $X$  into sets  $X^{t=0}, \dots, X^{t=v_3}$  such that if  $i = (x^1, x^2, x^3) \in X^{t=l}$  then  $x^3 = l$ . Observe that the Markov chain visits the sets  $X^{t=0}, \dots, X^{t=v_3}$  cyclically. That is, if  $i \in X^{t=l}$  then, if there is a  $u$  such that  $p_{ij}(u) > 0$  then  $j \in X^{t=l+1}$  (here we use the convention  $v_3 + 1 \equiv 0$ ). Note that each of the sets  $X^{t=l}$  has  $v/(v_3 + 1)$  elements.

The algorithm is the following:

(i) Start with an initial guess for  $\lambda_1^{\star,n}, \lambda_2^{\star,n}$  denoted by  $\lambda_1^{0,n}, \lambda_2^{0,n}$  and values  $h_1^{0,n}(i), h_2^{0,n}(i)$ , for  $i \in X^{t=0}$ . Set  $k \leftarrow 0$ .

(ii) For  $l = v_3$  down to  $l = 1$ , for all  $i \in X^{t=l}$ ,  $s = 1, 2$  compute:

$$\mu^{k,n}(i) = \underset{u \in F(i)}{\operatorname{argmin}} \left[ \lambda_2^{k,n} g_1^n(i, u) - \lambda_1^{k,n} g_2^n(u) + \sum_{j \in X^{t=l+1}} p_{ij}(u) (\lambda_2^{k,n} h_1^{k,n}(j) - \lambda_1^{k,n} h_2^{k,n}(j)) \right], \quad (26)$$

$$h_s^{k,n}(i) = g_s^n(i, \mu^{k,n}(i)) + \sum_{j \in X^{t=l+1}} h_s^{k,n}(j) p_{ij}(\mu^{k,n}(i)) - \lambda_s^{k,n}, \quad (27)$$

where we use again the convention  $v_3 + 1 \equiv 0$ .

(iii) For  $i \in X^{t=0}$ ,  $s = 1, 2$ , compute:

$$\mu^{k+1,n}(i) = \underset{u \in F(i)}{\operatorname{argmin}} \left[ \lambda_2^{k,n} g_1^n(i, u) - \lambda_1^{k,n} g_2^n(u) + \sum_{j \in X^{t=1}} p_{ij}(u) (\lambda_2^{k,n} h_1^{k,n}(j) - \lambda_1^{k,n} h_2^{k,n}(j)) \right], \quad (28)$$

$$\tilde{h}_s^{k+1,n}(i) = g_s^n(i, \mu^{k+1,n}(i)) + \sum_{j \in X^{t=1}} h_s^{k,n}(j) p_{ij}(\mu^{k+1,n}(i)) - \lambda_s^{k,n}. \quad (29)$$

(iv) For  $s = 1, 2$ , compute:

$$\delta_s = \sum_{i \in X^{t=0}} \frac{h_s^{k+1,n}(i)}{v/(v_3 + 1)},$$

and update  $\lambda_s^{k,n}$ ,  $s = 1, 2$  as:

$$\lambda_s^{k+1,n} = \lambda_s^{k,n} + \frac{\delta_s}{v_3 + 1} \quad (30)$$

(v) For  $s = 1, 2$  and  $i \in X^{t=0}$ , compute:

$$h_s^{k+1,n}(i) = \tilde{h}_s^{k+1,n}(i) - \delta_s \quad (31)$$

(vi) Set  $k \leftarrow k + 1$  and go to Step (ii).

**Proposition 2.** Assume that  $\lambda_1^{\star,n}, \lambda_2^{\star,n}, h_1^{\star,n}, h_2^{\star,n}$  is a fixed point of the algorithm. Then, it is an optimal solution for problem (18).

*Proof:* To be a fixed point we should have  $\delta_s = 0$ , for  $s = 1, 2$ . Thus,  $\tilde{h}_s^{\star,n} = h_s^{\star,n}$  and (22)-(24) are satisfied.  $\square$

*Remark 6.* Value iteration schemes for periodic Markov decision processes were first proposed in Su (1972)<sup>28</sup>. Similar ideas were used for water reservoir operation scheduling in Wang et al. (1986)<sup>29</sup>. In a different formation a similar idea was applied in Hu et al. (2014)<sup>30</sup>, for energy arbitrage. The basic difference of the proposed algorithm is that it applies to ratio-cost problems.

## 5 | NUMERICAL RESULTS

In this section, we give some numerical results showing the applicability of the proposed methods on a quite detailed BESS model. Furthermore, we present the optimal control law for several values of the parameters indicating some non-obvious dependences.

### 5.1 | BESS Parameters

In this section we present some numerical results for the 192kWh system presented in Schimpe et al. (2018)<sup>31</sup>. The maximum charging and discharging rate is 1C, i.e., the battery charges or discharges fully in 1h. We assume that the BESS participates in the 15min intraday market. Thus, we choose the discretization interval  $\Delta t$  to be 15 min, and the maximum value for the control input  $u_m$  is 0.25.

The BESS consists of 19968 3.2V/3Ah cells organized in blocks, modules and racks, with total nominal open circuit voltage of  $V_{OC} = 665.6V$ . In total we have 208 battery cells in series and 96 in parallel (for more details see Schimpe et al. (2018)<sup>31</sup>). For simplicity, we assume that the open circuit voltage does not depend on the SoC, and it is always equal to its nominal value.

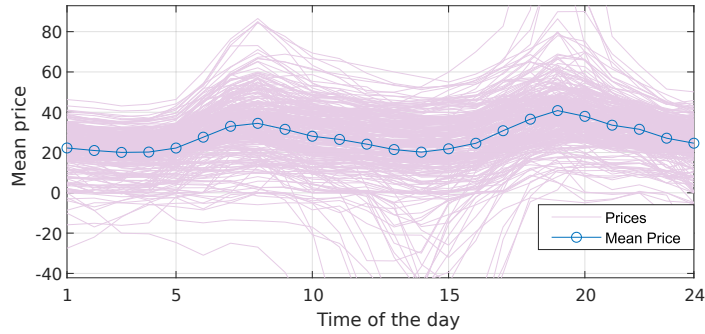


**FIGURE 3** The mean price as a function of the time-of-the-day. The diagram also presents the realized prices for the time interval under consideration. The mean price has two local minima at 3–4AM and 2–3PM and two local maxima at 8–9AM and 7–8PM.

The hysteresis voltage for a single cell is  $22mV$  and for the battery pack is  $V_h = 4.576V$ . The internal resistance for a single cell is approximately  $50m\Omega$  and thus for the BESS is  $R = 108.3m\Omega$ . Since, we assume that the current rating is  $1C$  the maximum current is  $3A \times 96 = 288A$  and the power rating is  $P^{\max} = 192kW$ .

Using Figure 9 of Schimpe et al. (2018)<sup>31</sup>, the power losses of the inverter are given by:

$$P_{\text{InvLoss}}(P_{\text{ib}}) = \begin{cases} 0.008P^{\max} + 0.017P_{\text{ib}}, & \text{if } P_{\text{ib}} \neq 0 \\ 0, & \text{if } P_{\text{ib}} = 0 \end{cases}. \quad (32)$$

In discrete time the model for the degradation  $g_2$  becomes:

$$g_2(x_k, Q_k, u_k) = (c_1^d + c_2^d x_k^1)Q^{-c_3^d} + |u_k|c_4^d Q^{-c_5^d} e^{c_6^d |u_k|}, \quad (33)$$

where the (discrete) parameters are given by:

$$\begin{aligned} c_1^d &= 4.5 \cdot 10^{-7}, & c_2 &= 6.6 \cdot 10^{-7}, & c_3^d &= 0.12, \\ c_4^d &= 5.9 \cdot 10^{-6}, & c_5^d &= 0.818, & c_6^d &= 1.62. \end{aligned}$$

We consider that the battery reaches the End of Life (EoL) when  $Q = 0.3$ .

*Remark 7.* The parameters for calendar aging are such that the battery will last for 15 years if it is empty and 6 years if it is full. The parameters for the cycling aging correspond to 3000 full cycles with  $1C$  rate, before the battery reaches the EoL. Furthermore,  $c_6^d$  is such that the battery degrades 1.5 times more for the same Ah, if the current is  $1C$ , compared to cycling with small current. These choices are consistent with the data presented in the literature<sup>32,33,34</sup>. The values of the exponents  $c_3^d$  and  $c_5^d$  are taken from Petit et al. (2016)<sup>7</sup>.

## 5.2 | Price Model Parameters

To calibrate the price model we use the publicly available data from the day-ahead DE-LU bidding zone from the first 9 months of 2020<sup>1</sup>. We assume that the BESS operates in the continuous market<sup>35</sup> with interval 15min, and that the day-ahead price data is a good approximation of the continuous market. For this data set, the mean hourly prices  $\bar{p}(t)$  are shown in Figure 3. The mean price for each time-of-the-day is computed as the average over the sampling period.

Having removed the seasonal trend  $\bar{p}(t)$ , to determine the parameters for the price model, we need to find the value of  $\alpha$  of the autoregressive model and the innovation distribution  $w_k$ . Discretizing this model we obtain the transition probability matrix. The details of the derivation of the 15min continuous market model are presented in the Appendix.

<sup>1</sup>This time period includes the first wave of COVID-19. We choose this period, because it has been argued that it offers a glimpse into the future power systems, where a high share of the consumed energy comes from renewable sources, e.g., <https://www.oxfordenergy.org/wpcms/wp-content/uploads/2020/07/COVID-19-GLIMPSES-OF-THE-ENERGY-FUTURE.pdf>

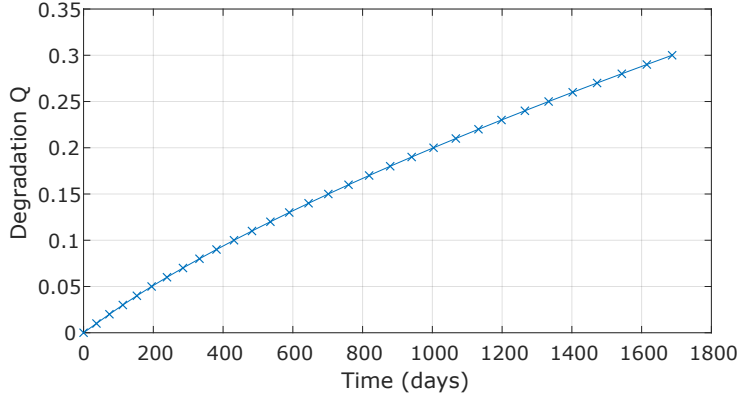


**FIGURE 4** The evolution of battery degradation over time. The data points are equally distanced vertically. That is, they correspond to degradation values  $0, 0.01, 0.02, \dots, 0.3$ . The curve in this figure is piecewise linear. The  $n$ -th line segment has slope  $\lambda_2^{\star,n}$ .

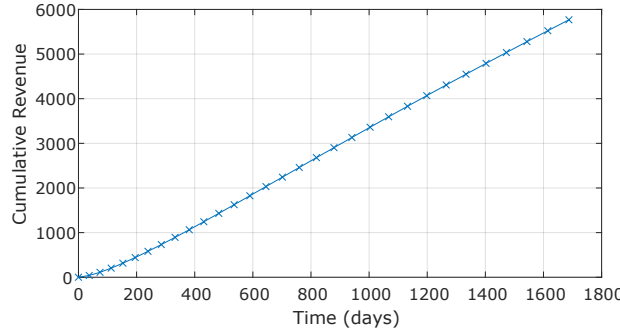


**FIGURE 5** The evolution of the cumulative revenue over time. The curve in this figure is piecewise linear. The  $n$ -th line segment has slope  $-\lambda_1^{\star,n}$ . The total revenue in the  $n$ -th interval is proportional to  $-\lambda_1^{\star,n}/\lambda_2^{\star,n}$ .

### 5.3 | Numerical Solution

We then use the algorithm of Section 4.2 to solve the optimal control problem with the parameters described in the previous subsections. Let us give some details of the discrete state space. The SoC state space  $X^1$  has 101 points, the price deviation state space  $X^2$  has 51 points and the time-of-the-day state space  $X^3$  has  $4 \cdot 24 = 96$  points. Thus, the state space of the fast variables  $X$  has  $v = 494496$  points. We use  $N = 30$  intervals for the discretization of  $Q$ .

Figures 4 and 5 illustrate the evolution of the battery degradation over time and the cumulative revenues over time, under the optimal control law. We observe that initially the battery degrades faster and that revenue rate increases as the battery gets older. Since the capacity of the battery becomes smaller as the degradation  $Q$  increases, we observe that it is optimal to use the battery more aggressively as  $Q$  increases.

Figure 6 shows the optimal trajectory of the SoC for a simulated trajectory of the price and three different values of  $Q$ . We observe that as the BESS becomes older, the optimal policy becomes more aggressive. We may observe in that in the last part of Figure 6 the BESS performs two full cycles almost every day.

*Remark 8.* Let us explain this finding. There are two competing phenomena. Buying energy below a price  $p_1$  and selling it back at a price  $p_2 > p_1$  is beneficial (ignoring temporarily the losses), but it increases the cycling aging of the battery. Thus, if there was no calendar aging, the BESS would expect a very high price spread  $p_2 - p_1$  to spend the remaining cycles, and would choose to remain idle for the most of the time. On the other hand as  $Q$  increases, calendar aging becomes more important, compared to the cycling aging. Thus, the battery degrades anyway, and this creates a pressure to act more frequently, even for smaller price margin  $p_2 - p_1$ .

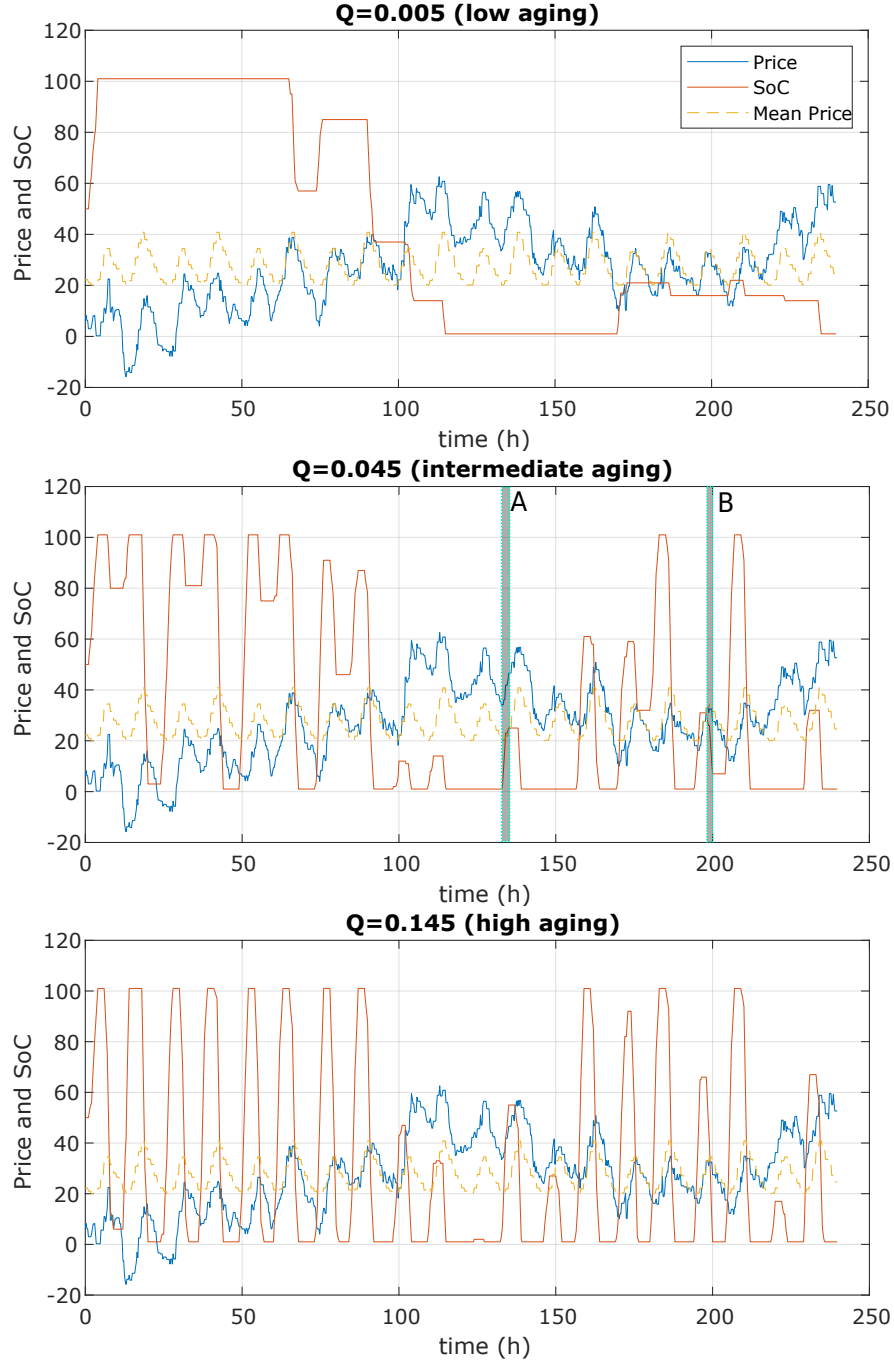


**FIGURE 6** The evolution of the SoC, for the same price signal, for three different values of  $Q$ . The price signal is a sample path of the stochastic model.

**Remark 9.** The optimal control action does not depend only on the price. From Figure 6, we observe that, indeed, in most cases, the BESS charges when the price is low and discharges when the price is high. However, comparing the gray regions A and B in the middle part of Figure 6, we observe that the BESS charges in region A at a higher price than the price in region B, where the BESS discharges. We may attribute this behavior to the time-of-the-day. Particularly, charging in region A starts at 2 pm, expecting that the price will increase. In contrast, in region B, the discharge begins slightly before 8 am, expecting that the price will decrease.

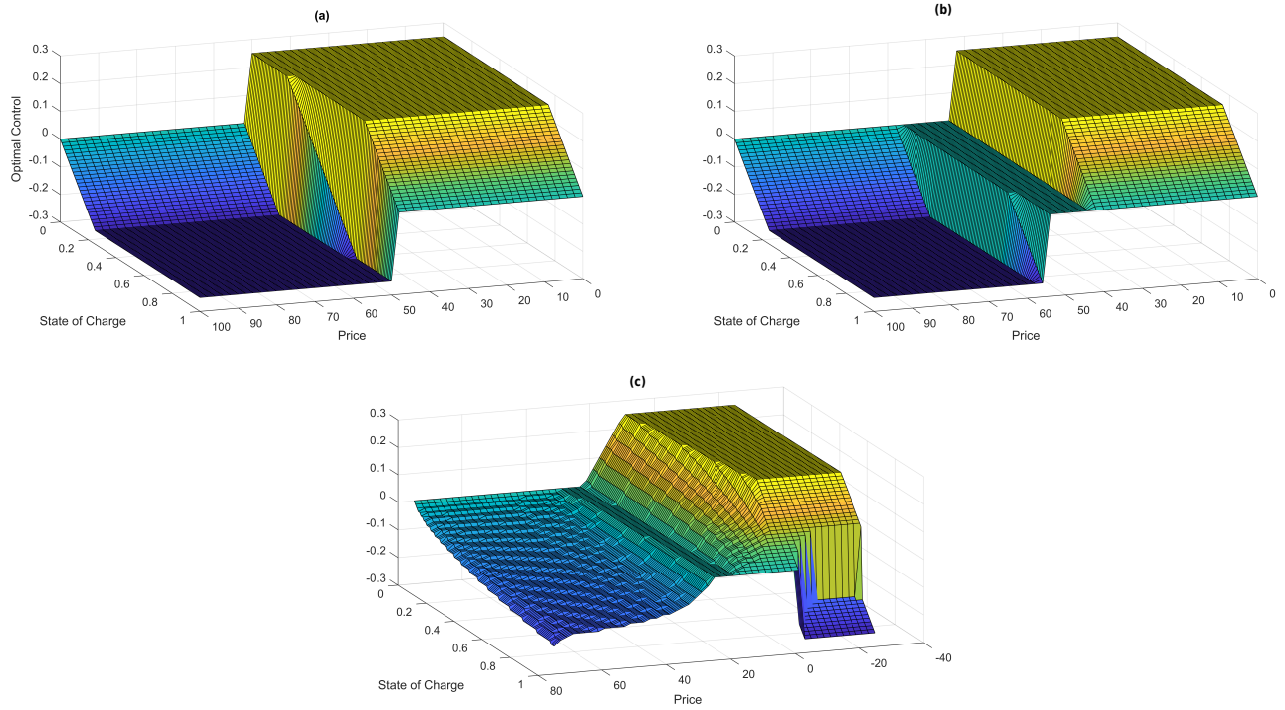


**FIGURE 7** The effects of price dynamics, and battery battery loss parameters on the optimal control law.

## 5.4 | The effects of the Model's Parameters on the Optimal Policy

In this subsection, we investigate the effect of the several model parameters on the optimal policy. To simplify presentation, we assume that there is no time-of-the-day effect i.e., the mean price  $\bar{p}(t_k)$  is a constant  $\bar{p}$ . At first we study the effects of the electrical parameters  $V_h$  and  $R$ , and the price dynamics and then move to the effect of the degradation parameters.

### 5.4.1 | The effect of Loss and Price Parameters

We start with the simplest possible model i.e., we assume that  $R = V_h = c_1^d = \dots = c_k^d = 0$  and that  $c_1^d = 1$ . In this case, aging is independent of the operational choices of the system. We further assume that  $\bar{p} = 50$ , that is the price is always positive and varies between 0 and 100. The optimal control law is shown in Figure 7.a. There are several regions. Whenever the price is above 50, the BESS sells the stored energy with the maximum possible power, constrained by the limits of the battery. Whenever the price is below 50, it absorbs energy with the maximum possible power constrained by the limits of the battery. Finally, when the price is exactly at 50, the BESS moves towards SoC 50% to improve the flexibility of future choices.

We then assume that the hysteresis voltage is positive  $V_h = 4.576V$  and the inverter losses are given by (32). The optimal control law is shown in Figure 7.b. The difference here is that there is a region of intermediate price, where the optimal operation for the BESS is to remain idle, i.e., not to absorb or release energy.

We then consider the effect of the internal resistance  $R = 0.1083\Omega$ . Additionally, the price varies between  $-25$  and  $75$ , i.e., we assume that price can take negative values, as well. Figure 7.c shows the optimal control law. Observe that when the price is low and the state of charge is high, the BESS discharges. The reason for this is that since the price is negative, and the expected price for the near future is negative as well, the BESS can cycle loosing some energy. But loosing some energy represents a profit, when the price remains negative. The existence of the internal resistance makes the optimal control law to vary smoothly with respect to the price (excluding of course the negative cycling region). This phenomenon has been also observed in Haessig (2020)<sup>36</sup>.

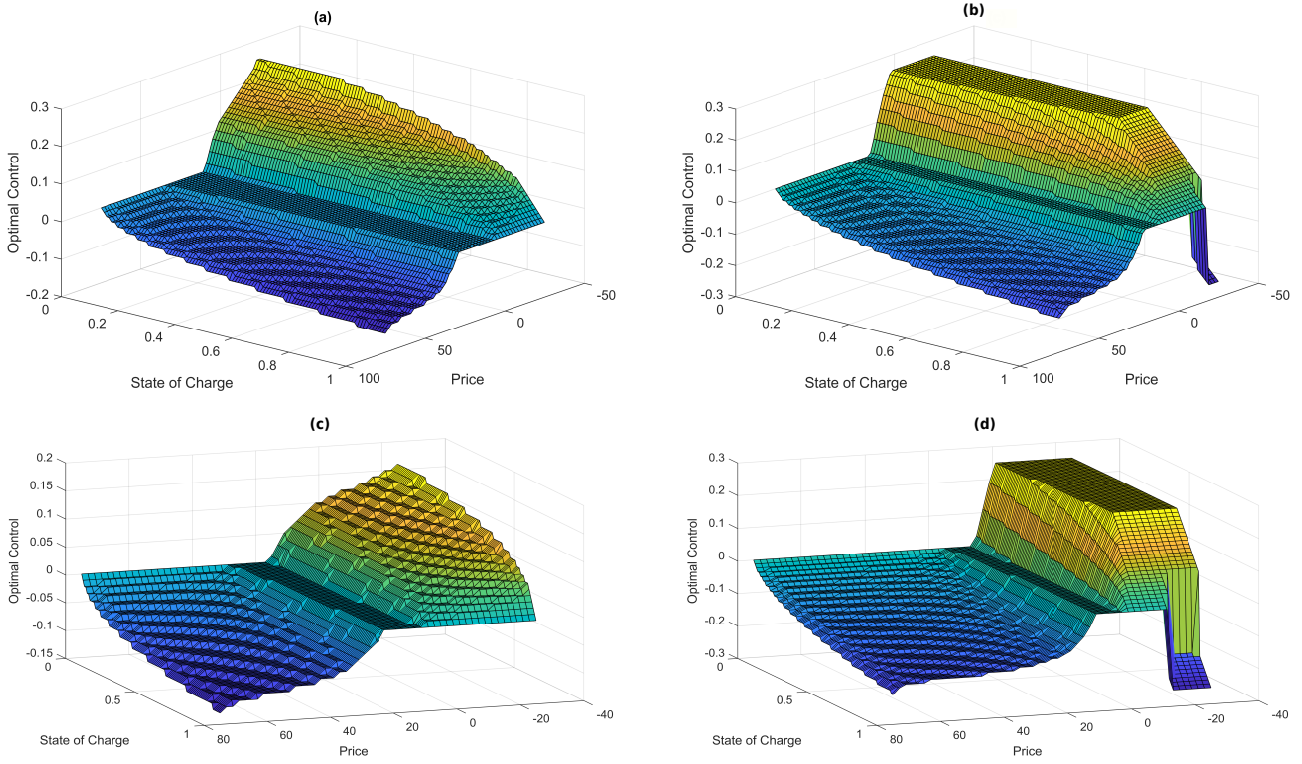


**FIGURE 8** Parts (a) and (b) present the effect of the degradation  $Q$  on the optimal control law. The value of  $Q$  is 0.01, and 0.3, respectively. Parts (c) and (d) illustrate the effect of the  $c_2^d$  and  $c_6^d$  parameters. Part (c) shows the optimal control law for  $c_6 = 6.48$  i.e., four times larger than the value of Subsection 5.1. Part (d) shows the optimal control law when  $c_2^d = 66$  i.e., 10 times more than before.

### 5.4.2 | The Effect of Degradation Parameters

We then investigate the effects of the degradation parameters on the optimal control law. Let us note that the degradation behavior of the batteries varies widely as a function of battery chemistry (e.g. Preger et al. (2020)<sup>26</sup>). Thus, this investigation is useful when choosing battery technology.

The degradation rate  $g_2$  can be written as:

$$g_2(x_k, Q_k, u_k) = Q^{-c_5^d} \left[ (C_1 + C_2 x_k^1) + |u_k| e^{c_6^d |u_k|} \right],$$

where  $C_1 = c_1^d Q^{c_5^d - c_3^d}$  and  $C_2 = c_2^d Q^{c_5^d - c_3^d}$ . Furthermore, the scale of the degradation rate  $g_2$  does not affect the optimal control law. Therefore, the optimal control law depends on three parameters  $C_1$ ,  $C_2$  and  $c_6^d$ . As the battery becomes older,  $C_1$  and  $C_2$  increase (recall that  $c_5^d > c_3^d$ ). The effects of the degradation  $Q$  on the optimal control law are illustrated in Figure 8 parts (a) and (b). As  $Q$  increases the calendar aging becomes more important. Furthermore, the optimal control law becomes more aggressive, the idle zone shrinks, and, at  $Q = 0.3$ , a negative cycling zone appears.

Figure 8.c shows the optimal control law for  $c_6^d = 6.48$ , i.e., four times larger than the value of Subsection 5.1. Recall that parameter  $c_6^d$  represents the extend to which the battery degrades faster when cycled with large currents. The effect of a higher  $c_6^d$  parameter is that the optimal control law varies less, and reaches its maximum power only when both the price and the SoC are low. Furthermore, the maximum power in this case is 0.16 (instead of 0.25). Figure 8.d shows the optimal control law when  $c_2^d = 66$  i.e., 10 times more than before, and the rest of the parameters are as in Subsection 5.1. Recall that parameter  $c_2^d$  represents the extend to which the battery degrades faster when remains idle with high SoC. We observe two qualitative differences here. First, the biggest price for which it is optimal to use  $u_k \geq 0$  goes from 15 to 7, that is, to charge the BESS, the price have to be lower. Thus, the average battery SoC is lower. Second, a negative cycling region appears. Negative price cycling is more attractive, when  $c_2^d$  is high, because it causes  $x_k^1$  to temporarily decrease.

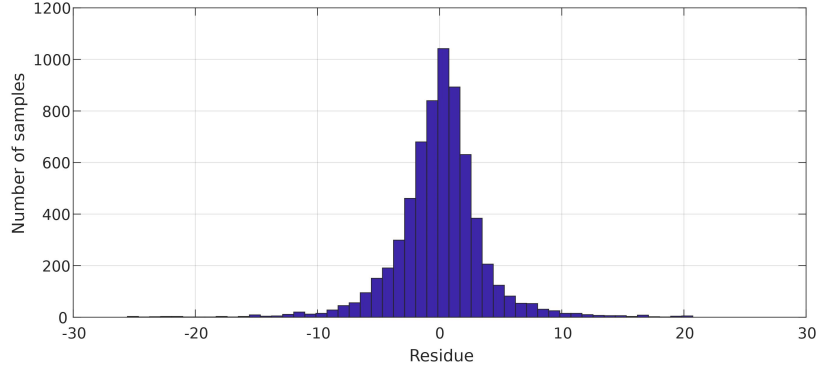


**FIGURE A1** The histogram of the residues.

## 6 | CONCLUSION

This paper dealt with the problem of maximizing the revenues obtained from a BESS over its lifetime, taking into account the effects of the control law on battery lifetime. The problem was transformed into a sequence of simpler ones, involving the minimization of the ratio of two long-time average-cost problems. We then derived a value-iteration-type algorithm for periodic problems with ratio costs. Numerical results indicate that as the battery becomes older, the optimal control law becomes more aggressive. We also investigated the effects of the electrical parameters (hysteresis, internal resistance, and the inverter losses) and the price dynamics parameters (mean price and variance) on the optimal control law.

In the future, we may consider more accurate models, including the increase of the internal resistance, nonlinear price models, and include fixed costs or discounting.



## APPENDIX

### A PRICE MODEL

There are many ways to generate a model for the 15 min market price. In this section, we present a model that is statistically consistent with the 1h data. However, the methods described in the main text may be applied to any such model.

Let us denote by  $\tilde{p}^{1h}(k)$  the deseasonalized price at hour  $k$ . We assume a first order linear model for the hourly price:

$$\tilde{p}^{1h}(k+1) = \alpha^{1h} \tilde{p}^{1h}(k) + w_k^{1h},$$

where  $w_k^{1h}$  are zero mean i.i.d. random variables. Using least squares, we estimate  $\alpha^{1h} = 0.9652$ . The histogram of the residues  $w_k^{1h} = \tilde{p}^{1h}(k+1) - \alpha^{1h} \tilde{p}^{1h}(k)$  is shown in Figure A1. We model the distribution of the hourly residues as a Laplace distribution with density:

$$f_{L,b}(z) = \frac{1}{2b} \exp\left(-\frac{|z|}{b}\right).$$

The maximum likelihood estimator for  $b$  is the mean absolute value of  $w_k^{1h}$ 's. For this data set  $b = 2.4681$ . The cumulative empirical distribution of the residues is compared with the cumulative of the Laplace distribution in Figure A2. For comparison, the maximum likelihood estimate of the Normal distribution is also plotted. It turns out that the Laplace distribution follows much more closely the empirical distribution compared to the Gaussian (e.g. in terms of the Kolmogorov–Smirnov statistic<sup>37</sup>). Let us note that Laplace distribution has been used in the literature for ARMA models (either as a marginal distribution<sup>38</sup>, or as the distribution of the innovation<sup>39</sup>).

We then use the model obtained for the hourly data to estimate a stochastic model for the 15min continuous market. The constant  $\alpha$  is given by:

$$\alpha = \alpha^{15\text{min}} = (\alpha^{1h})^{1/4} = 0.9912.$$

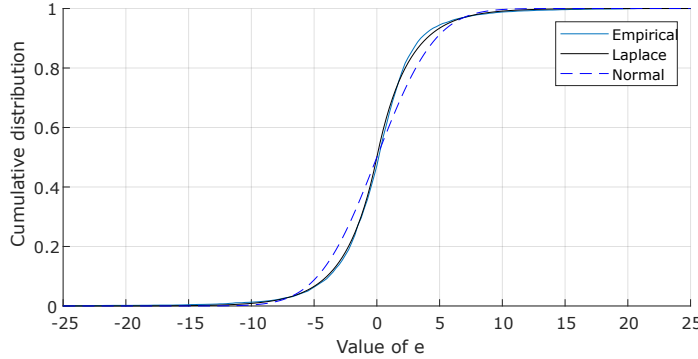


**FIGURE A2** The cumulative empirical distribution and the estimated cumulative Laplace distribution. For comparison, the maximum likelihood estimate of the Normal distribution is also plotted.

The probability density function  $f_w$  of  $w_k$  is such that the sum of four independent random variables  $w_k + \dots w_{k+3}$  (each  $w_i$  following  $f_w$ ) follows  $f_{L,b}$ . To find the distribution  $f_w$  we proceed as follows. First note that, for a random variable  $X$  following  $f_{L,b}$ , there are i.i.d. random variables  $X_+ \geq 0$  and  $X_- \geq 0$  such that  $X = X_+ - X_-$ , and  $X_+, X_-$  follow the exponential distribution with density  $f_E(z) = \frac{1}{b} \exp(-z/b)$ , for  $z \geq 0$  and  $f_E(z) = 0$ , for  $z < 0$ . The exponential distribution is infinitely divisible<sup>40</sup>. Thus, for the random variables  $X_+, X_-$ , there are i.i.d. random variables  $Y_+^1, \dots, Y_+^4$  and  $Y_-^1, \dots, Y_-^4$  such that  $X_+ = Y_+^1 + \dots + Y_+^4$  and  $X_- = Y_-^1 + \dots + Y_-^4$ , and  $Y_+^1, \dots, Y_+^4, Y_-^1, \dots, Y_-^4$  follow the Gamma distribution:

$$f_{\Gamma,b}(z) = \begin{cases} \frac{1}{\Gamma(1/4)b^{1/4}} z^{-3/4} e^{-z/b} & \text{if } z \geq 0 \\ 0 & \text{if } z < 0 \end{cases}.$$

Thus,  $X = Y^1 + \dots + Y^4$ , where  $Y^i = Y_+^i - Y_-^i$ . Therefore, the distribution  $f_w$  of  $w_k$  is given by the convolution  $f_w = f_{\Gamma,b} * f_{\Gamma,b}$ , i.e.:

$$f_w(z) = \int_{-\infty}^{\infty} f_{\Gamma,b}(\tau) f_{\Gamma,b}(\tau - z) d\tau.$$

## A.1 Discretization and Computation of the Markov chain

We then determine a model for the price Markov chain. The probability mass function for a discretized form of  $w$  is shown in Figure A3. The price is discretized in  $v_2$  intervals. Suppose that the price belongs to the  $i_2$  interval. We compute the probability distribution of the next price state  $\tilde{p}_{k+1}$  assuming that the current state  $\tilde{p}_k$  is distributed uniformly in the  $i_2$  interval. Then, we compute the distribution of the next state  $p_{k+1} = \alpha p_k + w_k$ . The distribution of the next state along with the distribution of

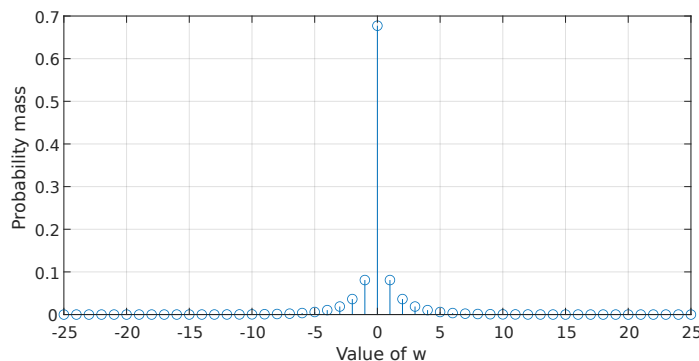


**FIGURE A3** The probability density function  $f_w$ .

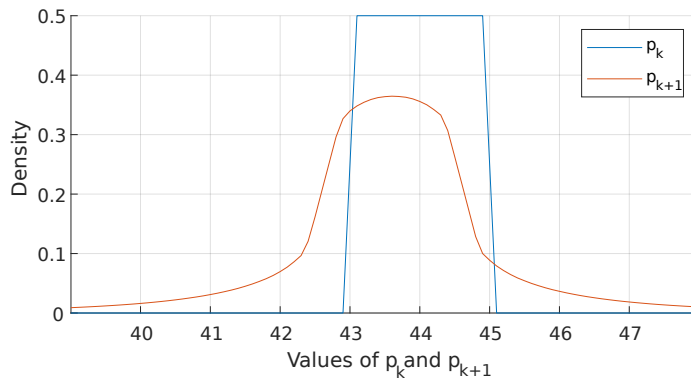


**FIGURE A4** The uniform distribution of the current state and the distribution of the next state. Observe that the next state has a mean closer to zero and it is more disperse due to the convolution with  $f_w$ .

the current state are illustrated in Figure A4. Finally, we integrate the density of  $p_{k+1}$  in each interval to compute the transition probability.

## References

1. Nykvist B, Nilsson M. Rapidly falling costs of battery packs for electric vehicles. *Nature climate change* 2015; 5(4): 329.
2. Curry C. Lithium-ion battery costs and market. *Bloomberg New Energy Finance* 2017; 5.
3. Vetter J, Novák P, Wagner MR, et al. Ageing mechanisms in lithium-ion batteries. *Journal of power sources* 2005; 147(1-2): 269–281.
4. Ramadass P, Haran B, Gomadam PM, White R, Popov BN. Development of first principles capacity fade model for Li-ion cells. *Journal of the Electrochemical Society* 2004; 151(2): A196–A203.
5. Safari M, Morcrette M, Teyssot A, Delacourt C. Multimodal physics-based aging model for life prediction of Li-ion batteries. *Journal of The Electrochemical Society* 2009; 156(3): A145–A153.
6. Reniers JM, Mulder G, Howey DA. Review and performance comparison of mechanical-chemical degradation models for lithium-ion batteries. *Journal of The Electrochemical Society* 2019; 166(14): A3189.
7. Petit M, Prada E, Sauvant-Moynot V. Development of an empirical aging model for Li-ion batteries and application to assess the impact of Vehicle-to-Grid strategies on battery lifetime. *Applied Energy* 2016; 172: 398–407.
8. Suri G, Onori S. A control-oriented cycle-life model for hybrid electric vehicle lithium-ion batteries. *Energy* 2016; 96: 644–653.
9. Barley CD, Winn CB. Optimal dispatch strategy in remote hybrid power systems. *Solar Energy* 1996; 58(4-6): 165–179.
10. Koller M, Borsche T, Ulbig A, Andersson G. Defining a degradation cost function for optimal control of a battery energy storage system. In: IEEE. ; 2013: 1–6.
11. Ying W, Zhi Z, Botterud A, Zhang K, Qia D. Stochastic coordinated operation of wind and battery energy storage system considering battery degradation. *Journal of Modern Power Systems and Clean Energy* 2016; 4(4): 581–592.
12. Shi Y, Xu B, Wang D, Zhang B. Using battery storage for peak shaving and frequency regulation: Joint optimization for superlinear gains. *IEEE Transactions on Power Systems* 2017.
13. Xu B, Shi Y, Kirschen DS, Zhang B. Optimal regulation response of batteries under cycle aging mechanisms. *arXiv preprint arXiv:1703.07824* 2017.

14. Díaz G, Gómez-Aleixandre J, Coto J, Conejero O. Maximum income resulting from energy arbitrage by battery systems subject to cycle aging and price uncertainty from a dynamic programming perspective. *Energy* 2018; 156: 647–660.
15. Haessig P, Ahmed HB, Multon B. Energy storage control with aging limitation. In: ; 2015.
16. Stroe DI, Knap V, Swierczynski M, Stroe AI, Teodorescu R. Suggested operation of grid-connected lithium-ion battery energy storage system for primary frequency regulation: Lifetime perspective. In: IEEE. ; 2015: 1105–1111.
17. Kazemi M, Zareipour H. Long-term Scheduling of Battery Storage Systems in Energy and Regulation Markets Considering Battery's lifespan. *IEEE Transactions on Smart Grid* 2017.
18. Carpentier P, Chancelier JP, De Lara M, Rigaut T. Algorithms for two-time scales stochastic optimization with applications to long term management of energy storage. 2019.
19. Heymann B, Martinon P, Bonnans F. Long term aging: an adaptative weights dynamic programming algorithm. 2016.
20. Carpentier P, Chancelier JP, De Lara M, Rigaut T. Time Blocks Decomposition of Multistage Stochastic Optimization Problems. *arXiv preprint arXiv:1804.01711* 2018.
21. Tan X, Wu Y, Tsang DH. A stochastic shortest path framework for quantifying the value and lifetime of battery energy storage under dynamic pricing. *IEEE Transactions on Smart Grid* 2017; 8(2): 769–778.
22. Tan X, Wu Y, Tsang DH. Pareto optimal operation of distributed battery energy storage systems for energy arbitrage under dynamic pricing. *IEEE Transactions on Parallel and Distributed Systems* 2016; 27(7): 2103–2115.
23. Kordonis I, Charalampidis AC, Haessig P. Optimal Control of MDPs over a Long Operation-Dependent Time Horizon and Application to Battery Energy Storage Systems. Submitted. Early version available online at <https://jkordonis.github.io/page/papers/BatteryRatio1.pdf>
24. Plett GL. *Battery management systems, Volume I: Battery modeling*. Artech House . 2015.
25. Santhanagopalan S, Smith K, Neubauer J, Kim GH, Pesaran A, Keyser M. *Design and analysis of large lithium-ion battery systems*. Artech House . 2014.
26. Preger Y, Barkholtz HM, Fresquez A, et al. Degradation of Commercial Lithium-Ion Cells as a Function of Chemistry and Cycling Conditions. *Journal of The Electrochemical Society* 2020; 167(12): 120532.
27. Bertsekas D. *Dynamic programming and optimal control*. Athena scientific Belmont, MA . 1995.
28. Su SY, Deininger RA. Generalization of White's method of successive approximations to periodic Markovian decision processes. *Operations Research* 1972; 20(2): 318–326.
29. Wang D, Adams BJ. Optimization of real-time reservoir operations with markov decision processes. *Water Resources Research* 1986; 22(3): 345–352.
30. Hu Y, Defourny B. Near-optimality bounds for greedy periodic policies with application to grid-level storage. In: IEEE. ; 2014: 1–8.
31. Schimpe M, Naumann M, Truong N, et al. Energy efficiency evaluation of a stationary lithium-ion battery container storage system via electro-thermal modeling and detailed component analysis. *Applied energy* 2018; 210: 211–229.
32. Sotta D. Final Report MAT4BAT. <https://cordis.europa.eu/docs/results/608/608931/final1-final-report-mat4bat-tables-and-figures.pdf> 2016.
33. Trad K, Govindarajan J. EVERLASTING: Report containing aging test profiles and test results. [https://everlasting-project.eu/wp-content/uploads/2020/03/EVERLASTING\\_D2.3\\_final\\_20200228.pdf](https://everlasting-project.eu/wp-content/uploads/2020/03/EVERLASTING_D2.3_final_20200228.pdf) 2018.
34. Schmalstieg J, Käbitz S, Ecker M, Sauer DU. A holistic aging model for Li (NiMnCo) O<sub>2</sub> based 18650 lithium-ion batteries. *Journal of Power Sources* 2014; 257: 325–334.

35. Viehmann J. State of the German short-term power market. *Zeitschrift für Energiewirtschaft* 2017; 41(2): 87–103.
36. Haessig P. Convex Storage Loss Modeling for Optimal Energy Management. 2020.
37. Corder GW, Foreman DI. *Nonparametric statistics: A step-by-step approach*. John Wiley & Sons. 2014.
38. Dewald L, Lewis P. A new Laplace second-order autoregressive time-series model–NLAR (2). *IEEE Transactions on Information theory* 1985; 31(5): 645–651.
39. Trindade AA, Zhu Y, Andrews B. Time series models with asymmetric Laplace innovations. *Journal of Statistical Computation and Simulation* 2010; 80(12): 1317–1333.
40. Billingsley P. *Probability and measure*. John Wiley & Sons. 2008. -